

In-Depth Practical Study of Length Metrology With Laser Interferometers Applying Different Techniques

Ihab H. Naeim

Taibah University, College of Sciences, Yanbu, Saudi Arabia
Length Metrology Division, National Institute of Standards, Egypt

Abstract:

The nanotechnology era or beyond always needs to develop and modernize methods of calibration and measurements considering the availability and benefit of applications. In this paper, I investigate two types of laser interferometers using two different techniques applying in Nano-metrology. In the tractability chain for Gauge Blocks length measurement, the PTB-Germany and NIS-Egypt are considered from the elites of national metrology institutes. A Double-Ended Interferometer being established in PTB as a traceable tool for other GB length interferometer (Single-Ended Interferometer). 10 steel GBs ranging in nominal length from 1.4 mm to 10 mm were calibrated in two accredited national laboratories applying two interferometric techniques. An absolute agreement between the measurement results was achieved. Reducing the uncertainty budget in SEI by eliminating the wringing process was the primary goal in designing the double-ended interferometer DEI. A detailed study and important results in this goal were achieved.

KEYWORDS: *Laser Interferometry, Double-ended interferometer, Phase correction, Uncertainty budget*

INTRODUCTION

Metrology science has become an important part of developing high-precision technologies (medical, industrial, military, etc.). All the accurate calibration techniques are focusing on one area (how to reach a zero error) in measuring techniques. Laser interferometer devices are one of the most precise measuring devices ever; an attempt was made to develop it by eliminating one of the difficult sources of error in measurement (wringing process) by changing the optical paths inside the interferometer dispense with wringing completely. Double-ended interferometer DEI has been constructed and developed in the national metrology institute of Germany (PTB). Single-ended

interferometer SEI and DEI are used at national metrology institutes NMI for linear dimensions calibration process based on the principle of laser interferometry. [1, 2] At NMIs, gauge blocks GB must be calibrated interferometrically with the smallest possible measurement uncertainties. Therefore, NMIs are placed at the top of the chain traceability of GB length measurement (accredited calibration national laboratories). The length of end standard (GB) is defined as the separation between its two flatten and highly polished faces. Depending on the degree of required accuracy, we select the measuring technique. We can optomechanically measure and calibrate the gauge blocks of different grades (K or 0) with high precision based on the well-known stabilized wavelengths (basic ruler) of laser sources using an interferometer. I will focus on a real comparison between different interferometric techniques that are important in dimensional metrology. The technical progress in classical NMI interferometers was always combined with the idea of creating a double-ended interferometer which passes by different steps in different international labs, one of the designs by Kuriyama et al. in 2006. [3]

Due to the small size of an adhesive layer (wringing film), that is placed between the gauge block and an auxiliary platen and some complicated geometrical processes; the need to create a double-ended interferometer is greatly delayed. In 1993 UK scientists reported an accurate setup of DEI at the UK's National Metrology Institute (NPL). Calibration is defined as a reference measurement process that could compare the corresponding values realized by standards in the same environmental conditions with a unified global reference. For decades, to overcome the most technical problems in high precision measurement of gauge blocks (zero-degree) by using interferometry, a lot of inventions are achieved.

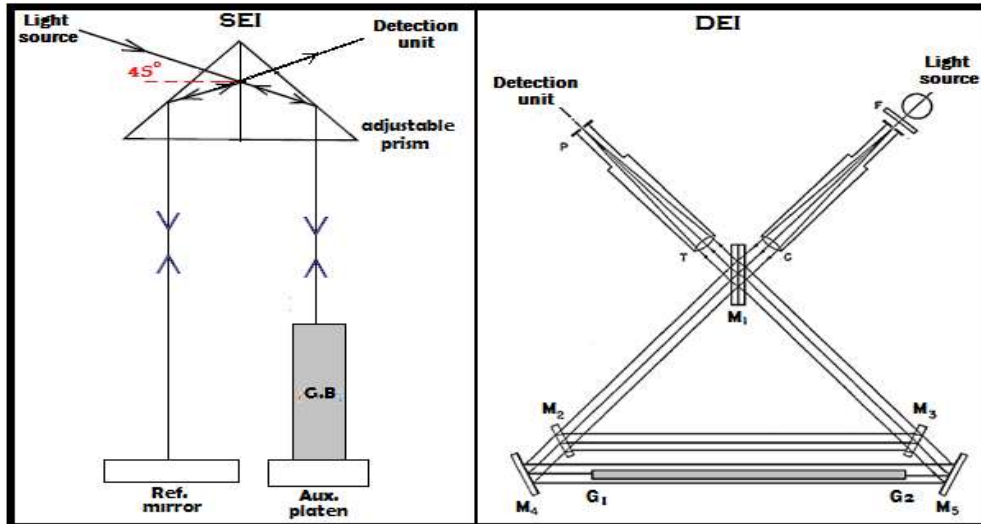


Figure 1, Schematic diagram of Köster interferometer-based Michelson theory (SEI & DEI); in 2nd part, c: collimator, T: telescope objective, M₁: beam splitter, M₂ & M₃: semi-reflecting mirrors, M₄ & M₅: mirrors, G₁&G₂: faces of GB.

Two interferometric techniques are accredited for end standard measurements in such degree or level [single-ended interferometer SEI and Double-ended interferometer DEI (fig.1)]. Due to the wringing process and its implications are affecting on the highly superfinishing gauge block surfaces. An advanced laboratory working in length metrology (PTB-Germany) established a new technique with an assumption that might measure end standards with zero error by completely avoiding the wringing process (Practically, zero error is not possible). [4]

Principle of length measurement by interferometry:

The following pathways are related to the measured interferograms and could be expressed in units of applied wavelengths.

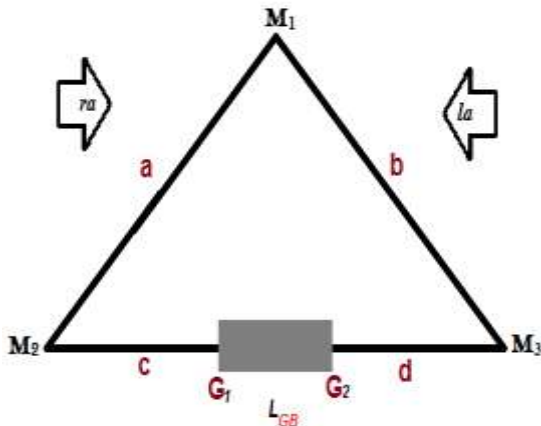


Figure 2, the geometrical optical path within DEI designed for measuring the accurate length of interior positioned GB.

$$L_1 = a + c + L_{GB} + d = \lambda_k [N_1 + (1/2\pi) \phi_{ra}] \quad (1)$$

$$L_2 = b + 2d = \lambda_k [N_2 + (1/2\pi) \phi_{ra}^{GB}] \quad (2)$$

$$L_3 = b + d + L_{GB} + c = \lambda_k [N_3 + (1/2\pi) \phi_{la}] \quad (3)$$

$$L_4 = a + 2c = \lambda_k [N_4 + (1/2\pi) \phi_{la}^{GB}] \quad (4)$$

N₁ to N₄ are integer orders, λ_k is the applied wavelength, and φ indicates average unwrapped phase values of the indices ra (right arm), la (left arm). According to the geometrical optical path and from these equations, the length of a GB is:

$$L_{GB} = [L_1 - L_2 + L_3 - L_4] / 2 \quad (5)$$

$$L_{GB} = \frac{\lambda_k}{2} \left\{ i_k + \underbrace{\frac{1}{2\pi}(\phi_{ra} - \phi_{ra}^{GB})}_{q_k} + \underbrace{\frac{1}{2\pi}(\phi_{la} - \phi_{la}^{GB})}_{q_k} \right\} \quad (6)$$

An integer order and q_k are the fractional order of interference (sum of fractional orders obtained from interferogram analysis in the right and left arms of DEI). The equivalent optical distance of space between gauge block ends G₁G₂ is accurately measured using laser

$$L_{GB} = \frac{\lambda_k}{2} (i_k + q_k)$$

interferometer as $K = 1, 2, ..$ (7)

L_{GB}: length being measured

q_k: is a fraction [0 to 1] λ_k/2

λ_k: is the wavelength used in the measurement.

$$\lambda_k = \frac{\lambda_o}{n_k}$$

In this, n_k is the computed refractive index affecting the applied wavelength, taking all the ambient parameters into consideration. The refractive index of the surrounding air in and out of the measuring chamber of an interferometer along optical paths can be accurately

computed by installing many electronic programable thermometers and hygrometer in parallel to the stabilization required to measurement process; by applying an empirical dispersion formula such as the updated Edlen's equation or Ciddor's equation together

with sensing of the ambient parameters. [5] These methods are known as capable of estimating the true value of the refractive index of air with uncertainties near a $\sim 10^{-8}$ level in well-controlled homogeneous laboratory conditions (Table 1).

| Parameter | Increment | Sensitivity |
|-------------------------|-----------|-------------------------|
| Temperature | 1 °C | -9.20×10^{-07} |
| Atm. Pressure | 1 Pa | 2.70×10^{-09} |
| CO ₂ content | 1 ppm | 1.44×10^{-10} |
| R.H | 1 % | -2.98×10^{-08} |

Table 1, the effecting environmental parameters on calibration processing for end standards internationally

Based on the provided information of T°, P (atmospheric pressure), R.H (relative humidity), and CO₂ content, we could easily compute n_k . Phase correction should be applied to the measured length of GB in the DEI because of the phase change on reflection at the two GB surfaces and its surface roughness. For light traveling in the air, the phase change on reflection δ is given as:

$$\delta = \text{ArcTan}.[2\kappa / 1 - n^2 - \kappa^2] \quad (8)$$

K is the extinction coefficient in the reflecting medium and n the refractive index of the reflective medium's refractive index. Typical length equivalent values for the phase change on reflection of steel, which is obtained by multiplying half of the wavelength, are summarized in table 2 (last column). [6, 7]

| Wavelength nm | n | κ | $(\lambda/2) \cdot \delta$ nm |
|---------------|-----|----------|-------------------------------|
| Green 532 | 1.9 | 3.2 | -19.56 |
| Red 633 | 2.2 | 3.4 | -20.94 |

Table2, typical values for n,k, and for the corresponding length equivalent phase on reflection found for steel.

Therefore, in DEI, the light on both sides of the gauge block appears to be reflected ~ 20 nm inside each end surface, even if the surface is perfectly smooth. The roughness of the test surface is proportional to the square root of the ratio between the diffused light and the reflected light of the GB surface.[8] The phase

correction in DEI is larger than it in SEI when the GB is wrung to an auxiliary platen. The corrections for the surface roughness and the phase change on reflection are often combined into one correction defined as "phase correction."

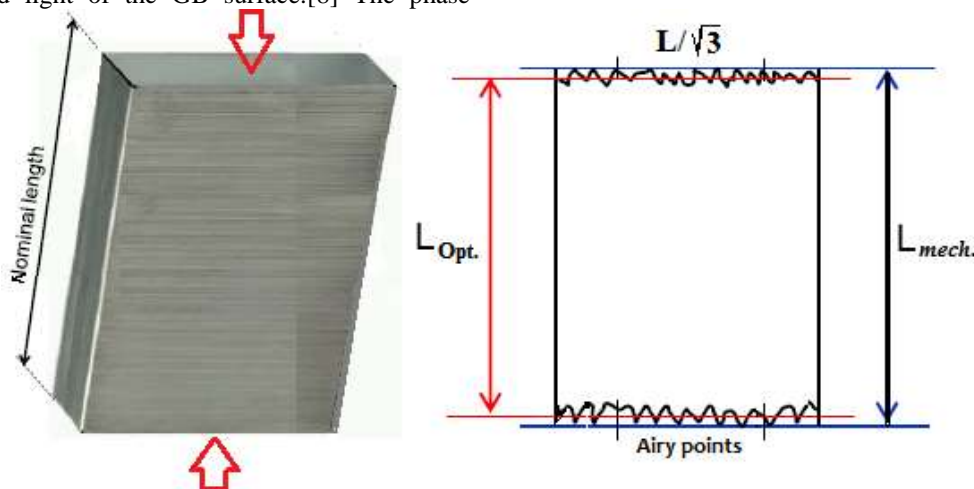


Figure 3, Schematic diagram for the difference between optical and mechanical length measurements of gauge blocks according to the degree of accuracy required.

The GB is placed horizontally inside the interferometer between the 2nd and 3rd beam splitter plates (fig. 2). GB'd supported at two specific named Airy points ($L/\sqrt{3}$). Without arguing the GB at an Airy point, the measuring process will be suffering from prismatic

compression under the effect of GB weight when standing vertically or from sagging when lying horizontally. The nominal length of GBs over 100 mm is important to support horizontally at two specific apart points (Airy points), each at 0.211 times the nominal

length from the GB ends. The length correction programmed equation at 20°C is:

$$L_{20^{\circ}\text{C}} = L_T [1 + \alpha_0 (20 - T)] \quad (9)$$

In which, L_T : measured length at $T \pm 20^{\circ}\text{C}$, and α_0 : Thermal expansion coefficient of the gauge block material. A gauge block of 1m steel platen being with a typical thermal expansion coefficient $1.2 \times 10^{-5} \text{ K}^{-1}$ will be measured about 1.2 μm longer at $T = 20.1^{\circ}\text{C}$ than at $T = 20.00^{\circ}\text{C}$. Then a highly accurate measurement of temperature is very important.

The resulting uncertainty can be estimated as:

$$U = \sqrt{(11.6 \text{ nm})^2 + (1.6 \times 10^{-7} L)^2}$$

The expanded uncertainty ($k=2$) is:

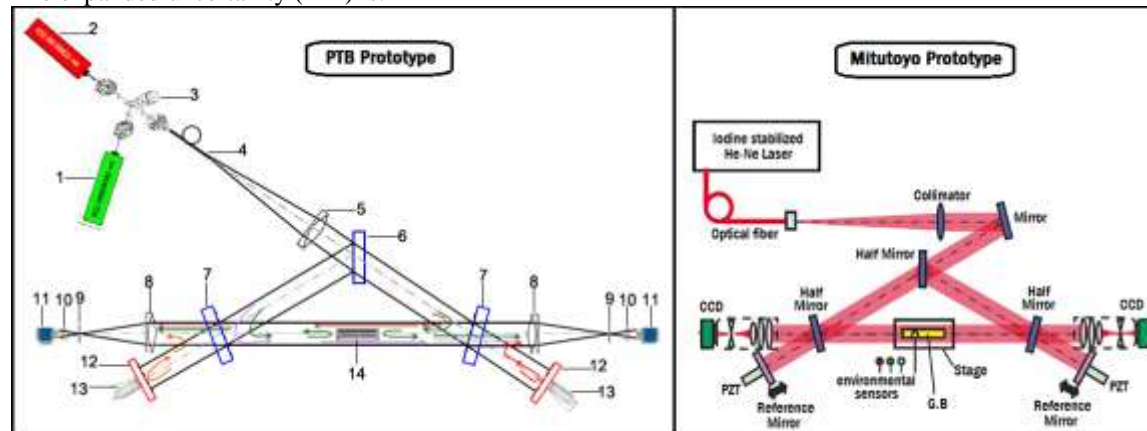


Figure 4, Schematic diagram of the PTB and Mitutoyo double-ended interferometers.

- 1-Iodine-stabilized frequency-doubled Nd:YAG laser. 2- Iodine stabilized He-Ne laser. 3- beam combiner with shutters. 4- single-mode fiber o/p. 5- beam collimator. 6,7- metal-coated beam splitter plates. 8- achromatic lenses. 9- o/p apertures. 10- o/p collimators. 11- CCD cameras. 12- reference mirrors. 13- piezo actuators. 14- GB.

A similar DEI built-in PTB uses more than laser stabilized wavelengths, making it more accurate and more effective in calibration methods. An optical modification that enables double-ended interferometer (DEI) to be more applicable to such a single-ended interferometer (SEI) for short or long gauge blocks is achieved. The correction for the surface roughness and the phase change on reflection are often combined into a single correction termed "phase correction." A procedure for evaluating the wave-front correction for different parts of the interferogram of DEI, and software have the capability for a nine-point phase stepping was designed. Accurate measurements of air temperature, atmospheric pressure, and humidity are essential for highly precise calculation of the refractive index n based on the empirical Edlén equation. The resolution of the temperature measurements is 1 mK, the atmospheric air pressure is measured with accuracy $\pm 8 \text{ Pa}$, Humidity is measured with a sensor accuracy of $\pm 1 \text{ \%RH}$, and the last effected parameter on n which is the CO_2 content (30 ppm) uncertainty. [10, 11] Only a few gauge blocks per set need testing to obtain phase

$$U = 2 \cdot \sqrt{(11.6 \text{ nm})^2 + (1.6 \times 10^{-7} L)^2}$$

The PTB Double-Ended Interferometer:

Building the first DEI equipped with CCD-cameras and phase stepping interferometric computation is accomplished in the laboratory of a gauge block manufacturer (Mitutoyo Co., Japan). It was built mainly for quality control of the production process of GBs. [9] The principle of laser interferometry enables the calculation of phasing and differences in optical path length due to the grade of surface finishing and length of gauge blocks in the measuring system.

correction. SEI & DEI results with different phase correction determination methods are presented and evaluated. The estimate of uncertainty for GB calibration with DEI gives a similar standard uncertainty to with the best SEIs, [4, 12]

$$U = \sqrt{(10.0 \text{ nm})^2 + (118 \times 10^{-9} L)^2}$$

Practically, for 10, 100, 300 mm steel GBs, the length measured by DEI at 20.0°C by applying the given data into the programmed equations: the phase correction for the 10 mm GB is 42 nm, for 100 mm GB is 47 nm, and for 300 mm is 52 nm. One can say the differences between these obtained results are due to the variations of surface roughness of these GBs. The repeatability is $< 3 \text{ nm}$.

The Single-Ended Interferometer:

Principle of Operation

It is based on the optical interference principle (Twyman-Green Type) to estimate the fringe fraction corresponding to the GB's length under calibration. The ray diagram of the Köster comparator is graphically illustrated in (figure 1-left side). Wringing is a technique by which the two applying surfaces are

gently adhered to seem as one mass by molecular attraction. The length of the GBs in the ambient conditions of measurement is then:

$$L = (N_1 + f_1) \cdot \lambda_1 / 2 = (N_2 + f_2) \cdot \lambda_2 / 2 \quad (10)$$

N: integer number

f: fringe fraction calculated from equation [a/b]

b: length between two successive fringes on reference plate; a: fringe fraction.

Applying the programable Benoit method of exact fraction serves for the direct computation of gauge block length. The fringe fraction is determined with accuracy $\lambda/20$. [13]

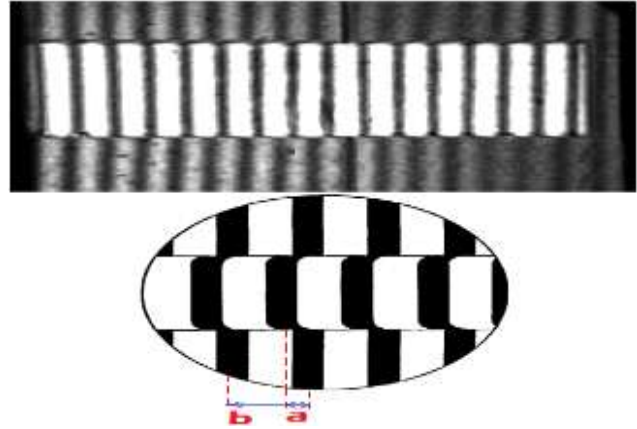


Figure 5, interference fringes captured by the CCD camera of the system.

| 1400 μm | 1500 μm | 2000 μm | 2500 μm | 3000 μm | 3500 μm | 4000 μm | 5500 μm | 6500 μm | 7000 μm |
|----------|----------|----------|----------|----------|----------|----------|----------|----------|----------|
| 1400.684 | 1499.948 | 2000.095 | 2500.008 | 2999.932 | 3500.131 | 4000.063 | 5500.073 | 6500.108 | 7000.274 |
| 1400.038 | 1499.952 | 2000.086 | 2499.997 | 2999.928 | 3500.120 | 4000.049 | 5500.065 | 6500.111 | 7000.280 |
| 1400.041 | 1499.949 | 2000.086 | 2499.998 | 2999.940 | 3500.115 | 4000.056 | 5500.065 | 6500.124 | 7000.279 |
| 1400.037 | 1499.961 | 2000.091 | 2500.010 | 2999.933 | 3500.120 | 4000.054 | 5500.070 | 6500.112 | 7000.270 |
| 1400.045 | 1499.955 | 2000.090 | 2500.003 | 2999.938 | 3500.130 | 4000.069 | 5500.065 | 6500.108 | 7000.266 |
| SD=0.004 | SD=0.005 | SD=0.004 | SD=0.006 | SD=0.005 | SD=0.007 | SD=0.008 | SD=0.003 | SD=0.008 | SD=0.005 |

Table 3, Gauge blocks calibrations using Köster interference comparator SEI.

In SEI, due to the wringing film thickness and the phase correction, there has a significant contribution to the total uncertainty with a deviation of up to 18 nm. In this technique, the contribution from the wringing film can be reduced to less than 10 nm.

As a result of multiple calibration times of gauge block (it can end up being wrung more than 20 times in its lifetime), it will affect the length of the gauge block described by Siddall. [14] He shows that wringing gauge blocks 50 times can result in a wringing variation of as high as 20 nm for steel gauge blocks.

| Uncertainty Sources | Estimated size | Standard uncertainty | Sensitivity coefficient | Uncertainty contribution $\times 10^{-9}m$ |
|-------------------------------------|---|--|---|--|
| laser stability | | $1.0 \times 10^{-9}m$ | L | 1.0L |
| Fringe Estimation | 0.006 fringe 1 fringe = 316.5 nm | $1.09 \times 10^{-9}m$ | 1 | 1.09 |
| Wringing film | | $7 \times 10^{-9} m$ | 1 | 7 |
| Roughness | | $3 \times 10^{-9}m$ | 1 | 3 |
| Flatness and parallelism | | $2 \times 10^{-9} m$ | 1 | 2 |
| Phase - change | | $8 \times 10^{-9} m$ | 1 | 8 |
| Optics flatness | $\pm 9 \times 10^{-9}$ | 5.2×10^{-9} | L | 5.2 L |
| Obliquity | $\pm 10 \times 10^{-9}$ | 5.77×10^{-9} | L | 5.77 L |
| Source Size | $\pm 15 \times 10^{-9}$ | 7.2×10^{-9} | L | 7.2 L |
| Sensor to Air | $\pm 0.01 \text{ } ^\circ C$ | $11.54 \times 10^{-3} \text{ } ^\circ C$ | $9.5 \times 10^{-7} L$ | 5.6 L |
| Sensor to Gauge block | $\pm 0.01 \text{ } ^\circ C$ | $5.77 \times 10^{-3} \text{ } ^\circ C$ | $\alpha L =$ $11.6 \times 10^{-6} LC^{-1}$ | 67 L |
| Variation of Temperature | $\pm 0.005 \text{ } ^\circ C$ | $5.77 \times 10^{-3} \text{ } ^\circ C$ | $(9.5 \times 10^{-7} + \alpha)L$ | 36.21L |
| Thermal exp. coefficient variations | $\pm 5\% \times \alpha$ $0.58 \times 10^{-6} \text{ } ^\circ C^{-1}$ | $0.33 \times 10^{-6} \text{ } ^\circ C^{-1}$ | $(T-20) L$ $0.05L \text{ } ^\circ C m$ | 16.73 L |

| Ambient Resolution of Instruments | | | | |
|-----------------------------------|--------------|------------------------------|----------------------------|--------|
| GB Temperature | ± 0.01 °C | 5.77 × 10 ⁻³ °C | α L | 67L |
| Temperature | ± 0.01 °C | 5.77 × 10 ⁻³ °C | 9.5 × 10 ⁻⁷ L | 5.48L |
| Air (PRT) | | | | |
| Pressure | ± 0.005 mbar | 2.88 × 10 ⁻³ mbar | 2.68 × 10 ⁻⁷ L | 0.77L |
| Humidity | 0.05 °C | 0.02885 °C | 34.6 × 10 ⁻⁹ L | 0.996L |
| CO ₂ content | 50 ppm | 57.7 ppms | 0.254 × 10 ⁻³ L | 7.375L |

Table 4, sources of uncertainty in SEI and its results

The main contribution to the lower total uncertainty has been made in the uncertainty components attributed to the fringe fraction estimation and analysis, evaluation of the refractive index of air and ambient wavelength, and gauge block temperature measurement.

$$U(\text{rep}) = 0.022 \mu\text{m} + 0.20 \times 10^{-6} \text{ L} \quad [3 \text{ wrings}]$$

The technical protocol of the comparisons was made according to the key comparison EUROMET. L-K1.1, calibration of GBs by interferometry, 2004. [2, 15]

Double-ended interferometry has several benefits like; there is no need for wringing, which scratches and

reduces the life of premium quality surfaces and requires expertise; there is improved repeatability. Some disadvantages of double-ended interferometry are that absolute phase change correction is needed for the gauge block, and its uncertainty has a double effect on total uncertainty in comparison with a single-ended interferometer. We apply two measurement techniques in order to distinguish the differences and, requiring for which one will be more appropriate in calibration processing with minimum sources of errors or uncertainty budget.

| Laser type | Vacuum wavelength (λ) nm | Standard Uncertainty nm | Refractive index |
|------------|--------------------------|-------------------------|------------------|
| Nd-YAG | 532.290008 | 7 × 10 ⁻¹² λ | 1.00026978 |
| He-Ne | 633.991398 | 5 × 10 ⁻¹¹ λ | 1.000268051 |

Table 5, The laser wavelengths, their standard uncertainties, and the refractive index of air according to the various ambient conditions.

The most important factors affecting the uncertainty budget in length metrology and have some differences obvious in the table below (Table 6).

| Interferometer | DEI | Köster |
|---|---|---|
| <i>Effecting factors in GB</i> | <i>Contribution to length Uncertainty</i> | <i>Contribution to length Uncertainty</i> |
| Wringing | 00 nm | 07 nm |
| Roughness | 10 nm | 07 nm |
| Phase change | 02 nm | 08 nm |
| Fringe fraction: λ₁(633 nm) | 3.2 nm | 3.2 nm |
| λ₂ (532 nm) | 2.1 nm | 2.1 nm |

Table 6. DEI & SEI standard uncertainty components (the factors differ) for steel GBs.

Considering all the provided information, one can conclude the combined standard uncertainty equation for double-ended interferometer as:

$$U = \sqrt{(12 \text{ nm})^2 + (0.13 \times 10^{-6} \text{ L})^2}$$

The standard uncertainty of the results of measurement is expressed as a standard deviation. A coverage factor, k, is typically in the range 2 to 3. It is used as a multiplier of the combined standard uncertainty to obtain an expanded uncertainty. [16]

Conclusion

In this study of different interferometric techniques, I found that, although avoiding the complicated wringing process in SE interferometer by changing the interior optical path to directly and accurately estimate the length of end standard at the reflection, only a few nanometers were the difference. When using DE

interferometer, the following should be considered: the budget of error due to the wringing process in SEI is surely less than the uncertainty budget due to the phase correction in DEI. i.e., the effect of phase change on reflection and surface roughness from both sides of the gauge block in the DEI is larger than in SEI. Based on a lot of reasons mentioned in this research work, I recommend using the SE interferometer commercially.

Acknowledgment

The author gratefully acknowledges the contribution of A. Abdelatty and Schödel (PTB-Germany) to this work.

REFERENCES

- [1] A.J. Lewis, “Absolute length measurement using multiple wavelength phase stepping interferometry”, Ph.D. Thesis, London University (1993).
- [2] International Vocabulary of Basic and General Terms in Metrology, BIPM, IEC, IFCC, ISO, IUPAC, IUPAP, OIML, 1993.
- [3] P. Hariharan, D. Sen, “New Gauge Interferometer”, Journal of the optical society of America, vol. 49, issue 3, pp 232-234, (1959).
- [4] A. Abdelaty, “Development of a double-ended gauge block interferometer for meas. of the absolute length”, PhD thesis, Technischen Universität Braunschweig, (2012).
- [5] G. Bonsch, J.R. Potulski, “Measurement of the refractive index of air and comparison with modified Edlen’s formulae” Metrologia 35, 133-139, (1998).
- [6] Y. Kuriyama, Y. Yokoyama, Y. Ishii, J. Ishikawa, “Development of a new interferometric measurement system for determining the main characteristics of gauge blocks”, Annals of the CIRP vol. 55/1, (2006).
- [7] B. Karlsson, C. G. Ribbing, “Optical constants and spectral selectivity of stainless steel and its Oxides”. J. Appl. Phys. 53, Issue 9, (1982).
- [8] G. Bonsch, “Interferometric calibration of an integrating sphere for determination of the roughness correction of gauge blocks” Proc. SPIE 3477, 152-160, (1998).
- [9] Mitutoyo company, Gauge Block with Calibrated Coefficient of Thermal Expansion (CET), Catalogue No. E4334.
- [10] Testo company, “Stationary Measurement Solutions, Transmitters and monitoring systems”, (2011).
- [11] Ihab Naeim, S. H. Ali, “Surface imperfection and wringing thickness in uncertainty estimation of end standards calibration”, Optics and Lasers in Engineering 60, (2014).
- [12] Uncertainty and dimensional calibration, J. Res. Natl. Inst. Stand. Technol. 102, (1997).
- [13] Weckenmann A., et al, “Manufacturing Metrology- State of the Art and Prospects”, 9th intern. symposium on measurement and quality control, 2007.
- [14] G. J Siddall et al, “Some Recent Developments in Laser Interferometry”, Optical Metrology 131, (1987).
- [15] BIPM, “Evaluation of measurement data-guide to the expression of uncertainty in measurement”, JCGM 100: (2008).
- [16] T. Youshizawa, “Handbook of optical metrology”, Tokyo: CRC Press, (2009).
- [17] Benjamin, Alina, "Measurable Characterization of the Slight Force Transducer used in Nano indentation Tools" SSRG International Journal of Applied Physics 3.3 (2016): 19-23.